Quantitative characterization of turbulence in an optical experiment

G. Steinmeyer, A. Schwache, and F. Mitschke
Institut für Angewandte Physik, Corrensstrasse 2/4, 48149 Münster, Germany
(Received 19 December 1995)

Experimental data from a turbulent optical system are analyzed quantitatively. The system consists of a nonlinear fiber ring resonator synchronously driven by a train of picosecond light pulses. Spatiotemporal dynamics reshapes the pulses and generates intricate substructure; its complexity can be chosen through choice of parameters. We extend standard procedures of time series analysis and show how a measure of the degree of complexity can be retrieved from the data. [S1063-651X(96)04905-7]

PACS number(s): 42.56.Sf, 42.65.Re

In recent years several approaches have been reported in order to obtain quantitative analytical tools for the evaluation of complexity in turbulent, i.e., spatiotemporally chaotic, systems [1–4]. To test these ideas, it would be desirable to have a system in which the number of participating spatial degrees of freedom can be controlled. Theoretical studies on arrays of coupled chaotic maps [1] do have this advantage, plus the bonus of computational efficiency. However, they seem to be somewhat remote from real world experimental situations.

We have recently described [5] an experimental system, from nonlinear optics, that can produce optical turbulence. A remarkable feature is that this turbulence occurs in only one spatial dimension. It was also shown [6] that the number of spatial degrees of freedom in this system can be set as desired. In this paper we will show that a controlled transition from purely temporal to fully spatiotemporal dynamics can be performed. We can thus set the ''degree of complexity,'' in a sense to be specified below.

We gathered experimental data under conditions corresponding to different degrees of complexity, then subject them to time series analysis. We demonstrate that it is possible to extract quantitative information on the degree of complexity, even for the case of fully spatiotemporal dynamics.

The experiment consists of a nonlinear optical resonator formed by an optical fiber, the output light of which is fed back to its input. The resonator is synchronously driven by a train of picosecond laser pulses. Since a single-mode fiber is used, any transverse degrees of freedom are ruled out. The intensity-dependent index of refraction of the fiber, in combination with its group velocity dispersion and the repetitive interference at the input, gives rise to a rich dynamics. The setup is shown schematically in Fig. 1. A brief description will suffice here; further experimental details of the ring resonator can be found in [5].

As a light source we employ an additive pulse mode-locked Nd:YAG (yttrium aluminum garnet) laser [7, 8] emitting pulses of width $\tau_0 \approx 15$ ps at a wavelength of $\lambda = 1.32$ μm with a repetition rate of 82.4 MHz. Alternatively, a synchronously pumped NaCl:OH^- color center laser with a pulse width of $\tau_0 \approx 1$ ps at $\lambda = 1.45, \ldots, 1.7$ μm at the same repetition rate is used. Different polarization-maintaining fibers are employed in the experiment; their length is $L = 9.2$ m throughout. Together with the different wavelengths of the two lasers we have access to values of group velocity dispersion from $\beta_2 = -25\ \mathrm{ps}^2/\mathrm{km}$ to $\beta_2 = +11\ \mathrm{ps}^2/\mathrm{km}$ in the fiber. The amount of dispersion is of utmost importance here: it sets the correlation width in the pulse, $\tau_{\mathrm{corr}} \approx \sqrt{|\beta_2| L}$, or in other words controls how fine the pulse substructure can get [6]. We use the term ''system size'' S to indicate the number of spatial elements, given by total volume to correlation volume. In our one-dimensional optical system, this reduces to the ratio of pulse width to correlation width of the pulse substructure, $S = \tau_0 / \tau_{\mathrm{corr}}$. In our experiment, the system size can be easily varied by the proper selection of fiber dispersion and pulse duration.

The output of the nonlinear interferometer is monitored by a fast photodiode. In addition, we detect the optical second harmonic, generated by a nonlinear crystal, to discriminate signal contributions from dynamical processes at pulse center from those in the wings (compare [5]). Both detector signals are digitized and stored by a digital storage oscilloscope. The sampling clock of this device is directly synchronized with the optical pulse train of the mode-locked laser. A third channel of the oscilloscope is used to monitor the pulse train at the interferometer input. This enables us to reject data sets in which any irregularities of the input, such as relaxation oscillations of the laser, are apparent. Using this setup we can record time series of pulse energies with lengths up to 2 Mbytes if required.

The data thus acquired have a very good signal-to-noise ratio; this was demonstrated through the observation of subharmonic period 32 behavior [5, 9]. Due to the high repetition rate, we can acquire as many as $n = 20\,000$ data points in a mere millisecond. Thus the influence of thermal parameter drift is expected to be of minor importance. Nevertheless, we confirmed stationarity with the technique of recurrence plots [10].

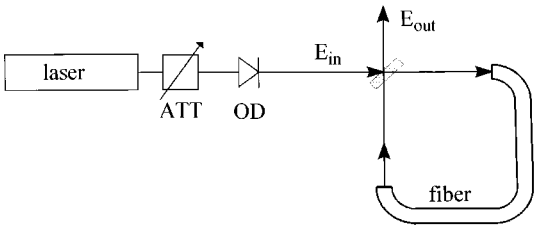

FIG. 1. Experimental setup. ATT: variable attenuator; OD: optical diode (Faraday rotator and polarizers).

Several procedures are known to detect nonlinear correlations in measured time series. One of the most succesful of these is an algorithm to compute the correlation dimension originally put forward by Grassberger and Procaccia [11] (GPA for short in this paper). It makes use of an embedding of the measured time series in an artificial phase space of dimension m, performs a statistical evaluation of distances of point pairs in this embedding space, and returns a function $D_2(m)$. If $D_2(m)$ converges, i.e., becomes independent of m at least for large m, that value is usually considered as the estimate for the correlation dimension.

However, there are several subtle problems with this algorithm: It can tolerate only a very limited amount of noise in the data, and it requires very long time series. In particular, the requirements on sample size grow exponentially and thus get excessive and impractical for anything higher in dimension than the simplest chaotic attractors. Basing an optimistic estimate on [12], one finds that the GPA is limited to something like $D_2<12$ for $n=10^6$. On the other hand, 10^6 data points are an upper limit of what is practical because computing time scales in proportion to n^2 and thus gets excessive: Using a widespread implementation [13] on a state-of-the-art work station an analysis of a data set with that sample size might easily exceed a CPU month.

Even if one has a sufficient number of data points the results of the GPA may still be ambiguous. The algorithm is sensitive to all kinds of correlations, and will also react to linear correlations; this may create the illusion of deterministic behavior in what really is colored noise. It is therefore of utmost importance to safeguard against such artifacts. It was pointed out in [14] that a comparison with so-called surrogate data, which have identical linear correlations as the measured data, allows the detection of determinism even in the case of noise-contaminated data. These data sets can be regarded as a stochastic rearrangement, or permutation, of the original data set. In this publication we use an algorithm that creates surrogates that have the identical histogram and very nearly the same power spectrum as the original [14].

Both original and a number of surrogate data sets are subject to GPA. This results in $D_2^{(\mathrm{orig})}$ and the average and the standard deviation for the surrogates, $\langle D_2{}^{(\mathrm{surr})}\rangle$ and $\sigma^{(\mathrm{surr})}$, respectively. The ''significance'' $\Sigma=(\langle D_2^{(\mathrm{surr})}\rangle - D_2^{(\mathrm{orig})})/\sigma^{(\mathrm{surr})}$ provides a measure of the difference between original and surrogates. A high value of the significance confirms the deterministic origin of the observed dynamics whereas for small Σ the deterministic origin of the data set should be rejected even in the case of convergence. This method was used to decide on the deterministic character of observed dynamics on many occasions [14,15]. (We note in passing that the generation of uncorrelated random numbers for surrogate generation is not trivial; here we use the subroutine RAN4 published in [16].)

We first consider experimental data taken at strong anomalous dispersion of $\beta_2=-23\ \mathrm{ps}^2/\mathrm{km}$ and with a relatively short pulse duration of $\tau_0=1.2$ ps. Figure 2 shows the result of the GPA analysis based on 16 384 data points. For the original, there is excellent convergence $D_2\to 2$ with increasing embedding dimension. At the same time, the corresponding surrogate data diverge, with Σ reaching values as high as 30. It is therefore reasonable to conclude that the observed behavior is due to determinism in the data and not due to an artifact of the GPA.

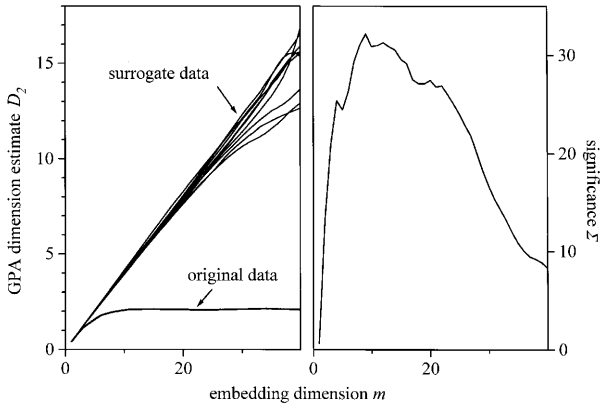

FIG. 2. Result of GPA analysis on a data set representing low-dimensional chaos. Left: Dimension estimate vs embedding dimension. Right: Significance (see text) vs embedding dimension. Conditions were $\tau_0=0.9$ ps and $\beta_2=-23\ \mathrm{ps}^2/\mathrm{km}$.

Next, let us consider data taken with much wider pulses ($\tau_0=15$ ps) and at a smaller value of (normal) dispersion ($\beta_2=7.4\ \mathrm{ps}^2/\mathrm{km}$). Under these conditions we find no convergence of the GPA but nevertheless values for Σ that range between 3 and 5.

We therefore attempt a procedure designed to improve the convergence behavior that was described in [4]. Since in a high-dimensional embedding space most data points lie close to the surface of the attractor (if it exists), the number of point pairs detected comes out systematically low. This can be corrected by using an analytic expression for the correlation sum for random numbers distributed in embedding space. Details can be found in [4]. We find that the correction seems to shift the limit set by the sample size to higher values: In this example, the dimension estimates are clamped at ≈ 11, which is just the value expected from [12]; with the correction the maximum is closer to 20. The correction is thus slightly helpful, and we will employ it in the remainder of this section.

It has also been used for Fig. 3. Still, both results from original and surrogates fail to converge and go up to values set by the sample size limit (left panel). However, the rate of divergence is significantly different for original and surrogate data ($\Sigma\approx 3.5$). Remarkably, the slope of $D_2^{(\mathrm{orig})}(m)$ is nearly constant. To better demonstrate this, the derivative $\delta=\partial D_2/\partial m$ is plotted in the right panel of Fig. 3.

If we further reduce dispersion to $\beta_2=0.25\ \mathrm{ps}^2/\mathrm{km}$ (Fig. 4), the difference between the divergence coefficient of the original and the surrogates is smaller but still statistically significant. Note, however, that now the slope $\delta\approx 0.66$ is steeper than before.

The failure of the GPA to converge indicates that additional degrees of freedom have been activated now. These additional degrees of freedom result from substructure formation in the pulses due to the much larger system size S. It has been argued [2,4,17] that in the case of spatially extended systems the attractor dimension is an extensive quantity; dimension divided by ''system size'' N (defined in [4] as the number of Lyapunov exponents; do not confuse with

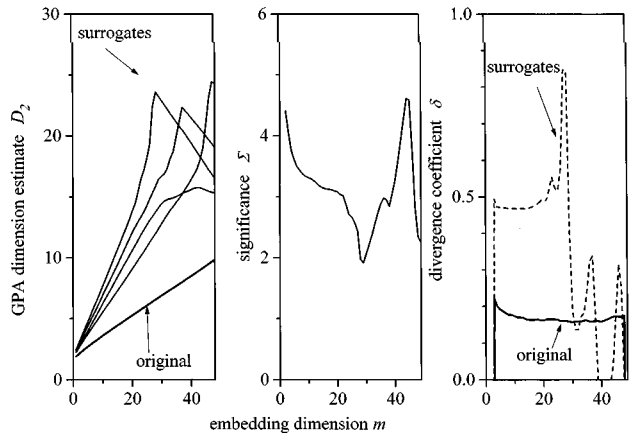

FIG. 3. Result of GPA analysis on a data set representing optical turbulence. Left: Dimension estimate vs embedding dimension; Middle: Significance (see text) vs embedding dimension; Right: divergence coefficient vs embedding dimension. Conditions were $\tau_0 = 15$ ps and $\beta_2 = 7.4\ \mathrm{ps}^2/\mathrm{km}$.

S defined above) would then give the dimension density, which would be size independent. Since N is also not known *a priori*, the dimension density ρ can be estimated as $\rho = D_2/m$ [4].

Formally, we follow this argument when we read the slope δ as above. Nevertheless, we emphasize that the physical situation is quite different here. In [4], embedding space is spanned either by time-shifted coordinates at a single spatial point $(x_t^{(1)}, x_{(t+\tau)}^{(1)}, \ldots, x_{(t+(m-1)\tau)}^{(1)})$, or by spatially shifted coordinates at one instant in time $(x_t^{(1)}, x_t^{(2)}, \ldots, x_t^{(m)})$. Here, we use time-shifted ensemble average values for embedding: $P_t, P_{t+\tau}, \ldots, P_{t+(m-1)\tau}$ where $P_{t+i\tau}$ is the total energy of the ith pulse, i.e., its power integrated over its duration. This corresponds to a summation over the spatial index. Keeping this distinction in mind, we prefer to call δ as used here the ''divergence coefficient.''

Evaluation of several experimental data sets, taken for differing values of dispersion, reveals that δ depends on the value of dispersion as well as on the input pulse width. It is highest for low dispersion and broad pulses. This is illustrated by Figs. 3 and 4.

Obviously, the GPA enhanced with surrogate analysis and the divergence coefficient is able to reproduce useful information on the degree of complexity even in the case of a fairly high number of degrees of freedom. δ can serve as a measure of complexity in the sense that it ranges from 0 to 1 when the number of spatial elements ranges from one to infinity. It is therefore a useful quantity to distinguish different degrees of turbulence and to measure complexity.

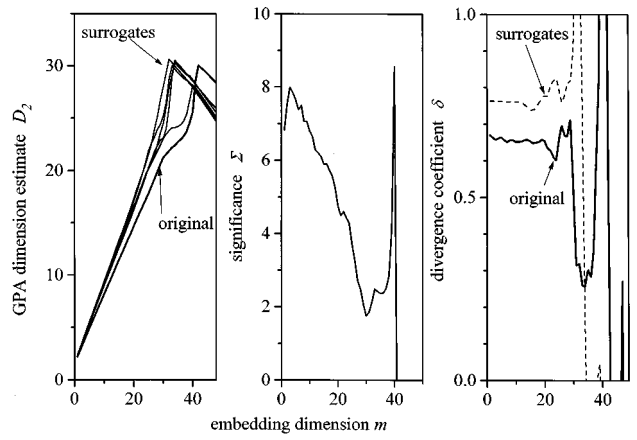

FIG. 4. Similar to Fig. 3, except for $\beta_2 = 0.25\ \mathrm{ps}^2/\mathrm{km}$.

The system size S (again, not to be confused with N as used in [4]) plays a role analogous to the Fresnel number in diffraction. For the data shown in Fig. 2 we estimate $S \approx 2$, whereas for those in Fig. 3 $S \approx 50$, and in Fig. 4 $S \approx 300$. While the latter value requires a downward correction to ≈ 200 once third-order dispersion is taken into account, the fact remains remarkable that determinism still can be traced from measured data.

We have reported on time series analysis on data from a system with a variable number of degrees of freedom. Our results indicate that even in the case of large (geometric) system sizes and in the presence of additional noise and parameter drift, as is typical for real experiments, traces of determinism in the data can well be detected from recordings of less than 20 000 data points. In several cases, we were able to obtain quantitative information from experimental data sets taken at $S \geqslant 100$.

Our method is an extension of the well-known GPA, which draws on surrogate analysis to safeguard against artifacts, on a correction to improve statistics at high embedding dimensions, and on concepts originally developed for the calculation of dimension density.

We consider it slightly surprising that the method is able to reveal this information in spite of the fact that we use ensemble averages, rather than pointwise measurements. While it has been shown mathematically [18] that a wide variety of transformations can be performed on measured data without topological distortion of the reconstructed phase space, the theorems involved require an embedding dimension at least twice the box-counting dimension of the attractor; we are in no way close to satisfying this requirement. Nevertheless, and in spite of all other imperfections that are characteristic for real world experimental data, the method produces useful information.

With the enhanced techniques described here we solve a long-standing problem that was first addressed by Ikeda theoretically [19] and Nakatsuka *et al.* experimentally [20]: To show with objective procedures from experimental data that there is chaotic (in fact, turbulent) dynamics in a nonlinear ring resonator.

The research described here has been performed in large part at the Institut für Quantenoptik of the University of Hannover with which the authors were affiliated until recently. We thank the head of that institute, H. Welling, for his encouragement. The computations presented in this paper were made possible by the use of the CAD/WAP workstation pool in the Department of Physics of the University of Hannover. We wish to express our thanks to H. Heng for fruitful discussions and for his assistance in giving us access to the program code described in [4]. We thank M. Kennel for running the ftp site lyapunov.ucsd.edu from which we downloaded an implementation of the GPA, GRASS-1.3. We gratefully acknowledge financial support by the Deutsche Forschungsgemeinschaft.

[1] K. Kaneko, Physica **23D**, 436 (1986).
[2] P. Grassberger, Phys. Scr. **40**, 346 (1989).
[3] M. B. Kennel and S. Isabelle, Phys. Rev. A **46**, 3111 (1993).
[4] M. Bauer, H. Heng, and W. Martienssen, Phys. Rev. Lett. **71**, 521 (1993).
[5] G. Steinmeyer, A. Buchholz, M. Hänsel, A. Schwache, and F. Mitschke, Phys. Rev. A **52**, 830 (1995).
[6] G. Steinmeyer and F. Mitschke, Appl. Phys. B **62**, 367 (1996).
[7] E. P. Ippen, H. A. Haus, and L. Y. Liu, J. Opt. Soc. Am. B **6**, 1736 (1989).
[8] F. Mitschke, G. Steinmeyer, M. Ostermeyer, C. Fallnich, and H. Welling, Appl. Phys. B **56**, 335 (1993).
[9] F. Mitschke, G. Steinmeyer, A. Buchholz, and M. Hänsel, in *Proceedings of the 2nd Experimental Chaos Conference*, edited by W. Ditto, L. Pecora, M. Shlesinger, M. Spano, and S. Vohra (World Scientific, Singapore, 1995), p. 53.
[10] J. P. Eckmann, S. O. Kamphorst, and D. Ruelle, Europhys. Lett. **4**, 973 (1987).
[11] P. Grassberger and I. Procaccia, Phys. Rev. Lett. **50**, 346 (1983); Physica D **9**, 189 (1983).
[12] D. Ruelle, Proc. R. Soc. London A **427**, 241 (1989).
[13] J. Goldberg, program code GRASS-1.3, Institute for Nonlinear Sciences, San Diego, CA; available at lyapunov.ucsd.edu.
[14] J. Theiler, B. Galdrikian, A. Longtin, S. Eubank, and J. D. Farmer, in *Nonlinear Modeling and Forecasting*, edited by M. Casdagli and S. Eubank, SFI Studies in the Sciences of Complexity Vol. XII (Addison-Wesley, Reading, MA, 1992), pp. 163–188; D. Prichard and J. Theiler, Phys. Rev. Lett. **73**, 951 (1994).
[15] M. Dämmig, G. Zinner, F. Mitschke, and H. Welling, Phys. Rev. A **48**, 3301 (1993).
[16] W. H. Press, B. P. Flannery, S. A. Teukolsky, and W. H. Vetterling, *Numerical Recipes in C. The Art of Scientific Computing* (Cambridge University Press, Cambridge, 1992), 2nd ed.
[17] G. Mayer-Kress and K. Kaneko, J. Stat. Phys. **54**, 1489 (1989).
[18] T. Sauer, J. A. Yorke, and M. Casdagli, J. Stat. Phys. **65**, 579 (1991).
[19] K. Ikeda, Opt. Commun. **30**, 257 (1979).
[20] H. Nakatsuka, S. Asaka, H. Itoh, K. Ikeda, and M. Matsuoka, Phys. Rev. Lett. **50**, 109 (1983).